

Numerical simulation of fracture waves in a blocky medium

V. M. Sadovskii, O. V. Sadovskaya



Institute of Computational Modelling SB RAS, Krasnoyarsk



Krasnoyarsk Mathematical Center

sadov@icm.krasn.ru, o_sadov@icm.krasn.ru



Conference **Dynamics in Siberia** 
March 2 - March 6, 2026

Fracture waves

The term “fracture wave” appeared in the 1960s, when a hypothesis about the principal possibility of the process of material fragmentation occurring in a relatively thin layer, propagating at a certain velocity, was put forward.

Among the first publications on the mathematical modelling of fracture waves are the works by J. D. Eshelby, G. I. Barenblatt, R. L. Salganik, G. P. Cherepanov, B. V. Kostrov.



Kanel' G. I., Molodets A. M., Dremin A. N. Investigation of singularities of glass strain under intense compression waves. *Combustion, Explosion, and Shock Waves*. 1977. Vol. 13, Iss. 6. P. 772–777. DOI: 10.1007/BF00740474



Rasorenov S. V., Kanel G. I., Fortov V. E., Abasehov M. M. The fracture of glass under high-pressure impulsive loading. *High Pressure Research*. 1991. Vol. 6, Iss. 4. P. 225–232. DOI: 10.1080/08957959108202508



Kanel' G. I., Zaretsky E. B., Rajendran A. M., Razorenov S. V., Savinykh A. S., Paris V. Search for conditions of compressive fracture of hard brittle ceramics at impact loading. *International Journal of Plasticity*. 2009. Vol. 25, Iss. 4. P. 649–670. DOI: 10.1016/j.ijplas.2008.12.004



Resnyansky A. D., Romensky E. I., Bourne N. K. Constitutive modeling of fracture waves. *Journal of Applied Physics*. 2003. Vol. 93, Iss. 3. P. 1537–1545. DOI: 10.1063/1.1534382



Cherepanov G. P., Esparragoza I. E. On self-sustaining fracture waves. *International Journal of Fracture*. 2007. Vol. 144, Iss. 3. P. 197–202. DOI: 10.1007/s10704-007-9090-5



Chaudhri M. M. Self-sustained fracture waves in soda-lime glass. *Materials Science Forum*. 2010. Vol. 662. P. 95–104. DOI: 10.4028/www.scientific.net/msf.662.95

Blocky structure of rocks

Many rocks have a blocky structure. Such a rock can be represented as a set of blocks, which has, according to acad. M. A. Sadovskii, the main distinguishing feature – the set of blocks is a hierarchically self-similar structure.

The blocky structure of the Earth's crust, revealed from the data of geological faults and studies of the propagation of seismic waves, has the following range of "predominant sizes": 10–12 km, 45–60 km, 100–120 km, 300–600 km.

Characteristic sizes of small-scale inhomogeneities: 4–6 m, 15–20 m, 150–250 m.

Despite the difference in the conditions of formation of rock types (sedimentary, volcanic), the main size of the "pieces" (separate blocks) is approximately 1.6–2 m.



Sadovskii M. A. Natural lumpiness of a rock. Dokl. Akad. Nauk SSSR. 1979. Vol. 247, Iss. 4. P. 829–831.

Preliminary stresses

The stress field arises as the result of sharp cooling of glass melt satisfies the **equilibrium equations** in Ω and the **free surface conditions** on Γ :

$$\frac{\partial \sigma_{ij}}{\partial x_j} = 0 \quad \text{in } \Omega, \quad \sigma_{ij} n_j = 0 \quad \text{on } \Gamma$$

σ_{ij} – components of the stress tensor

n_k – projections of the normal vector to the boundary

(summation over repeating indices; $i, j, k = 1, 2, 3$)

In the case of a spatial stress-strain state, self-balanced fields of prestresses can be constructed by specifying the **Airy stress functions**. There are three such functions U_k ; and using them, the **stress tensor components** are calculated by means of differentiation formulas:

$$\begin{aligned} \sigma_{11} &= \frac{\partial^2 U_3}{\partial x_2^2} + \frac{\partial^2 U_2}{\partial x_3^2}, & \sigma_{22} &= \frac{\partial^2 U_3}{\partial x_1^2} + \frac{\partial^2 U_1}{\partial x_3^2}, & \sigma_{33} &= \frac{\partial^2 U_2}{\partial x_1^2} + \frac{\partial^2 U_1}{\partial x_2^2} \\ \sigma_{12} &= -\frac{\partial^2 U_3}{\partial x_1 \partial x_2}, & \sigma_{13} &= -\frac{\partial^2 U_2}{\partial x_1 \partial x_3}, & \sigma_{23} &= -\frac{\partial^2 U_1}{\partial x_2 \partial x_3} \end{aligned}$$

Substituting these formulas into homogeneous equilibrium equations turns them into identities.

Preliminary stresses

The **free surface conditions** at the boundary Γ of domain Ω take the form:

$$\begin{aligned} \left(n_1 \frac{\partial}{\partial x_2} - n_2 \frac{\partial}{\partial x_1} \right) \frac{\partial U_3}{\partial x_2} + \left(n_1 \frac{\partial}{\partial x_3} - n_3 \frac{\partial}{\partial x_1} \right) \frac{\partial U_2}{\partial x_3} &= 0 \\ \left(n_2 \frac{\partial}{\partial x_3} - n_3 \frac{\partial}{\partial x_2} \right) \frac{\partial U_1}{\partial x_3} + \left(n_2 \frac{\partial}{\partial x_1} - n_1 \frac{\partial}{\partial x_2} \right) \frac{\partial U_3}{\partial x_1} &= 0 \\ \left(n_3 \frac{\partial}{\partial x_1} - n_1 \frac{\partial}{\partial x_3} \right) \frac{\partial U_2}{\partial x_1} + \left(n_3 \frac{\partial}{\partial x_2} - n_2 \frac{\partial}{\partial x_3} \right) \frac{\partial U_1}{\partial x_2} &= 0 \end{aligned}$$

These conditions are automatically satisfied if all three stress functions U_k are equal to zero at the boundary together with the first-order derivatives. More rigorously, it is sufficient to require that the derivatives $\partial U_k / \partial x_j$ take constant values at the boundary Γ .

Assuming that in the elementary volume of a glass melt, hardening in the absence of external stresses, the strain tensor is a spherical one, we obtain equations for calculating the self-balanced stress field from the **Castigliano variational principle**.

Taking into account the preliminary strain $\varepsilon_0(x_1, x_2, x_3)$, the **volumetric density of additional energy** in the linear elasticity theory is calculated by the formula:

$$\Psi = \frac{1}{4\mu} (\sigma_{11}^2 + \sigma_{22}^2 + \sigma_{33}^2) - \frac{\nu}{2E} (\sigma_{11} + \sigma_{22} + \sigma_{33})^2 + \frac{1}{2\mu} (\sigma_{23}^2 + \sigma_{13}^2 + \sigma_{12}^2) + \varepsilon_0 (\sigma_{11} + \sigma_{22} + \sigma_{33})$$

μ – shear modulus, ν – Poisson's ratio

$E = 2\mu(1 + \nu)$ – Young's modulus of the material



Preliminary stresses

The stress-dependent function Ψ is a strain potential, since the equations in potential form $\varepsilon_{ij} = \partial\Psi/\partial\sigma_{ij}$ correspond exactly to the constitutive equations of the linear theory of elasticity, taking into account the preliminary volumetric strain.

According to Castigliano's principle, the problem is reduced to **minimizing the integral**

$$I(U_1, U_2, U_3) = \int_{\Omega} \Psi(x_1, x_2, x_3) d\Omega$$

on the set of twice continuously differentiable functions, satisfying the free surface conditions on Γ .

Transformation of the **equations in variations**: $\delta_{U_1} I = \delta_{U_2} I = \delta_{U_3} I = 0$, characterizing the minimum of the integral, using Green's formula leads to the **Euler equations**, which correspond to the independent variations δU_1 , δU_2 и δU_3 :

$$\Delta_{23}^2 U_1 + (1 + \nu) \frac{\partial^2}{\partial x_1^2} \left(\frac{\partial^2 U_2}{\partial x_2^2} + \frac{\partial^2 U_3}{\partial x_3^2} \right) - \nu \Delta_{23} (\Delta_{13} U_2 + \Delta_{12} U_3) = -E \Delta_{23} \varepsilon_0$$

$$\Delta_{13}^2 U_2 + (1 + \nu) \frac{\partial^2}{\partial x_2^2} \left(\frac{\partial^2 U_1}{\partial x_1^2} + \frac{\partial^2 U_3}{\partial x_3^2} \right) - \nu \Delta_{13} (\Delta_{23} U_1 + \Delta_{12} U_3) = -E \Delta_{13} \varepsilon_0$$

$$\Delta_{12}^2 U_3 + (1 + \nu) \frac{\partial^2}{\partial x_3^2} \left(\frac{\partial^2 U_1}{\partial x_1^2} + \frac{\partial^2 U_2}{\partial x_2^2} \right) - \nu \Delta_{12} (\Delta_{23} U_1 + \Delta_{13} U_2) = -E \Delta_{12} \varepsilon_0$$

$\Delta_{ij} = \partial^2/\partial x_i^2 + \partial^2/\partial x_j^2$ – two-dimensional Laplace operators

Preliminary stresses

To simplify the situation with finding ε_0 , instead of constructing a complex physical and mechanical model of the formation of preliminary strain during the process of glass tempering, we introduce into consideration **three influence functions** defined by the equations $\theta_1 = \Delta_{23} \varepsilon_0$, $\theta_2 = \Delta_{13} \varepsilon_0$ and $\theta_3 = \Delta_{12} \varepsilon_0$. Summing these equations, we obtain $\Delta \varepsilon_0 = \theta$, where $\theta = (\theta_1 + \theta_2 + \theta_3)/2$.

We assume that the strain ε_0 is equal to zero at the boundary. Then for the solution of three-dimensional Poisson's equation with homogeneous boundary conditions on Γ , the **integral representation** (Green's formula) is valid:

$$\varepsilon_0(x) = \frac{1}{4\pi} \int_{\Omega} \frac{\theta(\xi)}{|x - \xi|} d\Omega - \frac{1}{4\pi} \int_{\Gamma} \frac{\theta_{\Gamma}(\xi)}{|x - \xi|} d\Gamma$$

$$x = (x_1, x_2, x_3), \quad \xi = (\xi_1, \xi_2, \xi_3), \quad \theta_{\Gamma} = \partial \varepsilon_0 / \partial n$$

Therefore, $\theta(\xi)$ is a function of influence of a particle at point ξ on the volumetric strain of a particle at point x .

Based on the **law of increasing entropy** (a measure of uncertainty of the distribution of preliminary strain over the volume of a material), we formulate the following **heuristic principle**.

The influence function, characterizing the distribution of preliminary strain during the process of glass melt hardening, should tend to a constant value, since such a tendency corresponds to the transition to complete uncertainty, i.e., chaos.

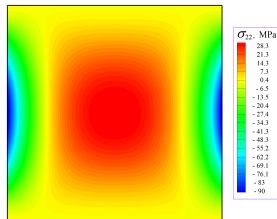
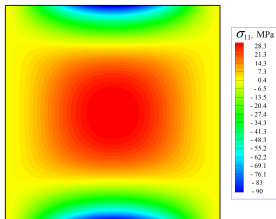
Thus, the influence function should minimize the integral:

$$J(\theta) = \int_{\Omega} |\nabla \theta|^2 d\Omega$$

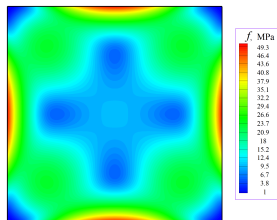
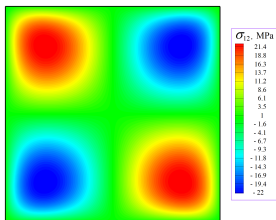
$$\nabla = (\partial/\partial x_1, \partial/\partial x_2, \partial/\partial x_3) - \text{the Hamilton operator}$$

Preliminary stresses

In a plane strain state the equation for Airy stress function with free-surface boundary conditions and a constant right-hand side describes the equilibrium of an elastic plate clamped at the edge under a uniformly distributed pressure. For a rectangular plate, the deflection function can be obtained using the separation of variables method in the form of a rapidly converging trigonometric series.



*Self-balanced fields
of stresses σ_{11} , σ_{22} , σ_{12}
and intensity of tangential
stresses $f(\sigma)$*

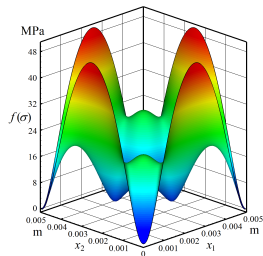
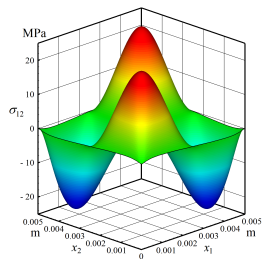
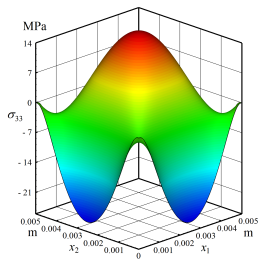
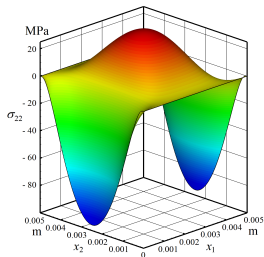
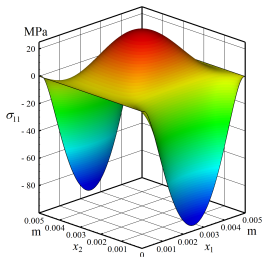


Intensity of tangential
stresses is reduced to
the yield point of glass
 $\tau_s = 50$ MPa.

Preliminary stresses

1 block 5 × 5 mm in size

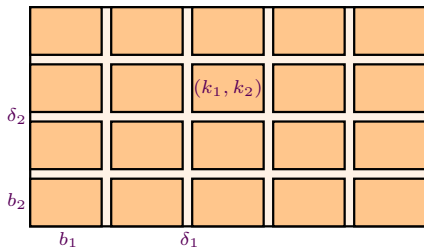
finite-difference grid in the block – 200 × 200 meshes



Level surfaces of stresses σ_{11} , σ_{22} , σ_{33} , σ_{12} and intensity of tangential stresses $f(\sigma)$



Equations of blocky elastic medium



Scheme of a blocky medium

A motion of each block is defined by the system of equations of dynamic theory of elasticity:

$$\rho \dot{v}_1 = \sigma_{11,1} + \sigma_{12,2}$$

$$\rho \dot{v}_2 = \sigma_{12,1} + \sigma_{22,2}$$

$$\dot{\sigma}_{11} = (\lambda + 2\mu) v_{1,1} + \lambda v_{2,2}$$

$$\dot{\sigma}_{22} = \lambda v_{1,1} + (\lambda + 2\mu) v_{2,2}$$

$$\dot{\sigma}_{33} = \lambda (v_{1,1} + v_{2,2})$$

$$\dot{\sigma}_{12} = \mu (v_{2,1} + v_{1,2})$$

Elastic interlayer between the horizontally located nearby blocks is described by the system of equations:

$$\rho' \frac{\dot{v}_1^+ + \dot{v}_1^-}{2} = \frac{\sigma_{11}^+ - \sigma_{11}^-}{\delta_1}, \quad \frac{\dot{\sigma}_{11}^+ + \dot{\sigma}_{11}^-}{2} = (\lambda' + 2\mu') \frac{v_1^+ - v_1^-}{\delta_1}$$

$$\rho' \frac{\dot{v}_2^+ + \dot{v}_2^-}{2} = \frac{\sigma_{12}^+ - \sigma_{12}^-}{\delta_1}, \quad \frac{\dot{\sigma}_{12}^+ + \dot{\sigma}_{12}^-}{2} = \mu' \frac{v_2^+ - v_2^-}{\delta_1}$$

Elastic interlayer between the vertically located nearby blocks is modeled using similar system:

$$\rho' \frac{\dot{v}_2^+ + \dot{v}_2^-}{2} = \frac{\sigma_{22}^+ - \sigma_{22}^-}{\delta_2}, \quad \frac{\dot{\sigma}_{22}^+ + \dot{\sigma}_{22}^-}{2} = (\lambda' + 2\mu') \frac{v_2^+ - v_2^-}{\delta_2}$$

$$\rho' \frac{\dot{v}_1^+ + \dot{v}_1^-}{2} = \frac{\sigma_{12}^+ - \sigma_{12}^-}{\delta_2}, \quad \frac{\dot{\sigma}_{12}^+ + \dot{\sigma}_{12}^-}{2} = \mu' \frac{v_1^+ - v_1^-}{\delta_2}$$

Elastic-plastic deformation of blocks

Under intensive mechanical impacts, the material of blocks turns into a plastic state. It is described by means of the variational inequality of the von Mises thermodynamic principle of the maximum power of plastic dissipation:

$$\begin{aligned}
 & (\tilde{\sigma}_{11} - \sigma_{11}) \left(\dot{\sigma}_{11} - \nu(\dot{\sigma}_{22} + \dot{\sigma}_{33}) - E v_{1,1} \right) + \\
 & + (\tilde{\sigma}_{22} - \sigma_{22}) \left(\dot{\sigma}_{22} - \nu(\dot{\sigma}_{33} + \dot{\sigma}_{11}) - E v_{2,2} \right) + \\
 & + (\tilde{\sigma}_{33} - \sigma_{33}) \left(\dot{\sigma}_{33} - \nu(\dot{\sigma}_{11} + \dot{\sigma}_{22}) \right) + \\
 & + (\tilde{\sigma}_{12} - \sigma_{12}) \left(2(1 + \nu) \dot{\sigma}_{12} - E(v_{1,2} + v_{2,1}) \right) \geq 0
 \end{aligned}$$

$\tilde{\sigma}_{j k}$ – varied stresses satisfying the constraint $f(\tilde{\sigma}_{j k}) \leq \tau_s$

f – material yield function, τ_s – yield point

$\nu = \lambda/2(\lambda + \mu)$ – Poisson's ratio, $E = 2\mu(1 + \nu)$ – Young's modulus

As a yield function we will use the intensity of tangential stresses by von Mises:

$$f = \sqrt{\frac{1}{6} \sum_{j>k} (\sigma_{jj} - \sigma_{kk})^2 + \sigma_{12}^2}$$

In this case, the numerical algorithm implementing the variational inequality is reduced to the well-known Wilkins stress correction procedure.



Elastic-plastic interlayers

To take into account the plasticity, constitutive equations of the vertical elastic interlayer are replaced by the variational inequality:

$$(\delta\sigma_{11}^+ + \delta\sigma_{11}^-) \dot{\varepsilon}_{11}^p + (\delta\sigma_{12}^+ + \delta\sigma_{12}^-) \dot{\varepsilon}_{12}^p \leq 0$$

$$\delta\sigma_{jk}^\pm = \tilde{\sigma}_{jk}^\pm - \sigma_{jk}^\pm \quad - \text{variations of stresses}$$

$$\dot{\varepsilon}_{11}^p = \frac{v_1^+ - v_1^-}{\delta_1} - \frac{\dot{\sigma}_{11}^+ + \dot{\sigma}_{11}^-}{2(\lambda' + 2\mu')}, \quad \dot{\varepsilon}_{12}^p = \frac{v_2^+ - v_2^-}{\delta_1} - \frac{\dot{\sigma}_{12}^+ + \dot{\sigma}_{12}^-}{2\mu'} \quad - \text{plastic strain rates}$$

The actual stresses σ_{jk}^\pm and admissible stresses $\tilde{\sigma}_{jk}^\pm$ are subjected to the constraint in the form:

$$f' \left(\frac{\tilde{\sigma}_{11}^+ + \tilde{\sigma}_{11}^-}{2}, \frac{\tilde{\sigma}_{12}^+ + \tilde{\sigma}_{12}^-}{2} \right) \leq \tau'_s(\chi)$$

τ'_s – material yield point of interlayers

χ – parameter (or set of parameters) of hardening

$f'(\sigma_n, \sigma_\tau)$ – equivalent stress function, in which arguments are normal and tangential stresses

The simplest form of the constraint for a microfractured medium (the Coulomb–Mohr condition) is as follows:

$$|\sigma_\tau| \leq \tau'_s - k'_s \sigma_n \quad (\tau'_s \text{ and } k'_s \text{ – phenomenological parameters of the material})$$

Constitutive equations of the horizontal elastic-plastic interlayer are formulated in a similar way.

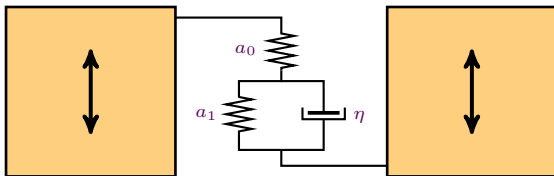


Accounting for viscosity and porosity of interlayers



Viscosity

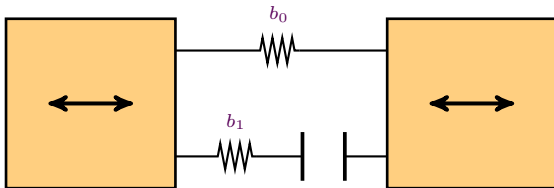
To describe the viscous dissipative effects in the interlayers under shear stresses, the Poynting–Thomson model of a viscoelastic medium is used.



Poynting–Thomson's rheological scheme

Porosity

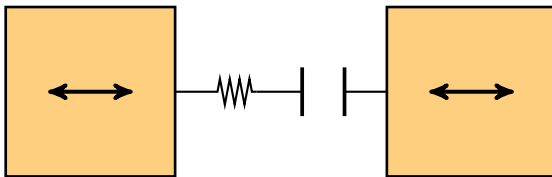
Deformation of interlayers is described on the basis of a complicated version of the porous elastic model, which takes into account the strength increasing during the collapse of pores.



Rheological scheme of a porous interlayer



Cracking of interlayers



Rheological scheme of contact interaction of crack edges

Conditions of contact interaction of the crack edges are formulated as a variational inequality:

$$\delta\sigma_{11} \left(\frac{1}{\rho' c_1'^2} \sigma_{11} - \varepsilon_{11} \right) \geq 0, \quad \dot{\varepsilon}_{11} = \frac{v_1^+ - v_1^-}{\delta_1}$$

The algorithm of numerical implementation in a mesh of finite-difference grid is based on the equations:

$$\hat{\varepsilon}_{11} = \varepsilon_{11} + \frac{v_1^+ - v_1^-}{\delta_1} \tau, \quad z_1 v_1^+ + \sigma_{11}^+ = R_1^+, \quad z_1 v_1^- - \sigma_{11}^- = R_1^- \quad \left(z_1 = \frac{\rho' c_1'}{\rho c_1} \right)$$

and the closing equation $\hat{\sigma}_{11} + \sigma_{11} = \sigma_{11}^+ + \sigma_{11}^-$, guaranteeing the absence of artificial dissipation of energy, which gives the procedure of stress correction:

$$\hat{\sigma}_{11} = \frac{1}{\kappa} \pi \left(\varepsilon_{11} + \frac{R_1^+ - R_1^- - \sigma_{11}}{z_1 \delta_1} \tau \right), \quad \kappa = \frac{1}{\rho' c_1'^2} + \frac{\tau}{\rho c_1 \delta_1}$$

Formation of cracks in rock samples

Laboratory experiments on axial compression of rock samples under the conditions of hydrostatic stress state show that, regardless of the magnitude of hydrostatic pressure p , the fracture of samples is accompanied by the formation of rupture cracks oriented along the axis.

The length of rupture cracks depends significantly on the pressure level and decreases with its increase.

At low pressures, long cracks prevent the development of shear cracks on the areas of maximum shear stress oriented at an angle of $\pi/4$ to the axis. At higher lateral pressures, when rupture cracks become short, macroscopic fracture occurs in the form of localized shear cracks.

Photographs of fractured cylindrical samples:



Fracture of rock samples under hydrostatic pressure

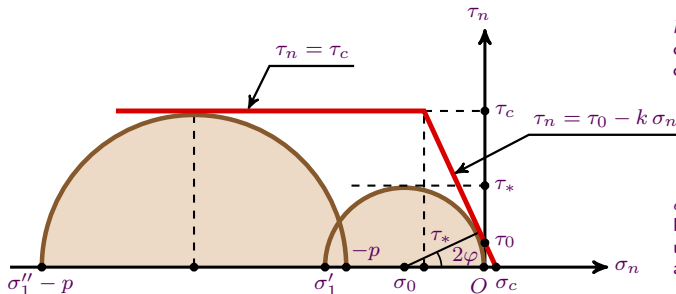


Tarasov B. G. Fan mechanism creating dynamic ruptures with high permeability at seismogenic depths of the Earth's crust. Russian Journal of Geophysical Technologies. 2024. No. 1. P. 118–186. DOI: 10.18303/2619-1563-2024-1-118



Coulomb – Mohr strength criterion

The simplest variant of the limit fracture curve – a two-link broken line (red line).



$k = \operatorname{tg} \alpha$ – angular coefficient of inclined link of the broken line

$$\varphi = \frac{\pi}{4} - \frac{\alpha}{2}$$

σ_c and τ_c – strength limits of the material under uniaxial tension and pure shear

Limit fracture curve on the Mohr diagram

In the absence of lateral stress, the large Mohr circle touches the inclined link of broken line. The point of contact corresponds to the area along which the crack develops.

As the pressure increases, the point of contact between the large circle and the limit curve moves up along the inclined link of broken line and passes to the horizontal link $\tau_n = \tau_c$, the points of which correspond to the areas of maximum shear stress, located at an angle of $\pi/4$ to the axis of sample.

The strength condition for the limit curve under consideration takes the form:

$$\tau_n = \begin{cases} \tau_c, & \text{if } \sigma_n < \sigma_0 \\ k(\sigma_c - \sigma_n), & \text{if } \sigma_n \geq \sigma_0 \end{cases}$$

$$\sigma_0 = \sigma_c - \frac{\tau_c}{k}$$



Two-cyclic splitting

We developed parallel computational algorithm for supercomputers of the cluster architecture based on a two-cyclic method of splitting, which permits the efficient parallelization of computations.

Governing equations in blocks and interlayers are represented in the form of symbolic evolution equation:

$$\dot{U} = A_1(U) + A_2(U)$$

A_1 and A_2 – nonlinear differential-difference operators, simulating 1D motion of a blocky medium in the direction of the coordinate axes x_1 and x_2

U – vector-function of unknown quantities, which includes the projection of the velocity vector and the stress tensor in blocks and interlayers

The method of splitting on the time interval $(t_0, t_0 + \Delta t)$ includes 4 steps:

- 1) the step of solving 1D equation in the x_1 direction on the interval $(t_0, t_0 + \Delta t/2)$
- 2) the step of solving 1D equation in the x_2 direction (similar to step 1)
- 3) the step of recomputation in the x_2 direction on the interval $(t_0 + \Delta t/2, t_0 + \Delta t)$
- 4) the step of recomputation in the x_1 direction on the same interval:

$$\dot{U}^{(1)} = A_1(U^{(1)}), \quad U^{(1)}(t_0) = U(t_0)$$

$$\dot{U}^{(2)} = A_2(U^{(2)}), \quad U^{(2)}(t_0) = U^{(1)}(t_0 + \Delta t/2)$$

$$\dot{U}^{(3)} = A_2(U^{(3)}), \quad U^{(3)}(t_0 + \Delta t/2) = U^{(2)}(t_0 + \Delta t/2)$$

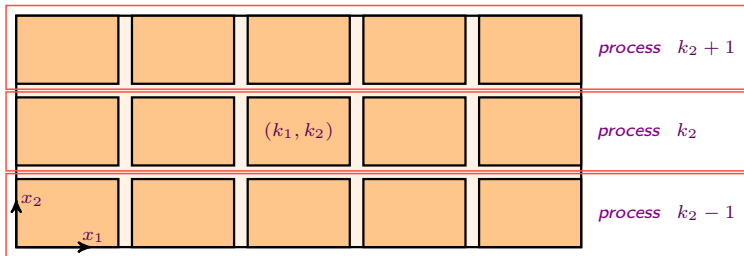
$$\dot{U}^{(4)} = A_1(U^{(4)}), \quad U^{(4)}(t_0 + \Delta t/2) = U^{(3)}(t_0 + \Delta t)$$

The solution at the time instant $t_0 + \Delta t$ equals to $U(t_0 + \Delta t) = U^{(4)}(t_0 + \Delta t)$

Parallel computational algorithm

Computational algorithm is implemented as a complex of parallel programs for **multiprocessor computing systems**.

The programming language is **Fortran**, and the message passing interface (**MPI**) library is used.



Distribution of computational load between parallel processes

Parallelization is performed on the basis of **1D domain decomposition** – each processor of a cluster serves a separate chain of blocks including the boundary interlayers in the horizontal direction.

In the vertical direction, **data exchange between processes** takes place.



Registration of program

Parallel program system
for numerical modeling of dynamic
processes in multi-blocky media
on cluster systems



*Program
2Dyn_Blocks_MPI*

Certificate of state registration of
computer program No. 2016615178
from 17.05.2016 (Rospatent)

Our recent publications



Sadovskii V. M., Sadovskaya O. V. Supercomputer Modeling of Wave Propagation in Blocky Media Accounting Fractures of Interlayers. In: *Nonlinear Wave Dynamics of Materials and Structures. Ser.: Advanced Structured Materials*. Vol. 122. Springer, Cham, 2020. P. 379–398. DOI: 10.1007/978-3-030-38708-2_22



Sadovskaya O. V., Sadovskii V. M. Mathematical modelling of fracture waves in a blocky medium with thin compliant interlayers. *Philosophical Transactions of the Royal Society. Ser. A: Mathematical, Physical and Engineering Sciences*. 2024. Vol. 382, Iss. 2277. Art. 20230305. DOI: 10.1098/rsta.2023.0305



Sadovskii V. M., Sadovskaya O. V. Application of Dynamic Model of a Blocky Medium to Describe the Plastic Deformation of a Structurally Inhomogeneous Material at the Mesoscale Level. In: *Mechanics and Acoustics of Metamaterials. Ser.: Advanced Structured Materials*. Vol. 245. Springer, Cham, 2026. P. 197–226. DOI: 10.1007/978-3-032-11462-4_13

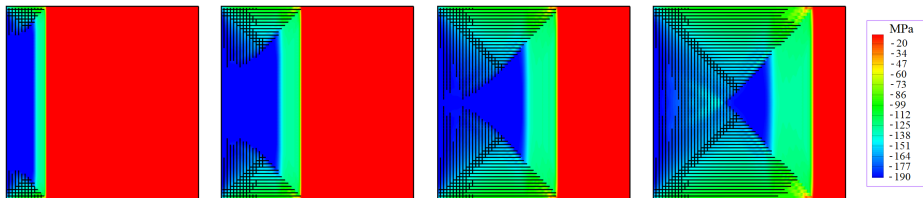


Садовский В. М., Садовская О. В. Численное моделирование волн разрушения в блочной среде // *Журнал вычислительной математики и математической физики*. 2026. Т. 66. 17 с.

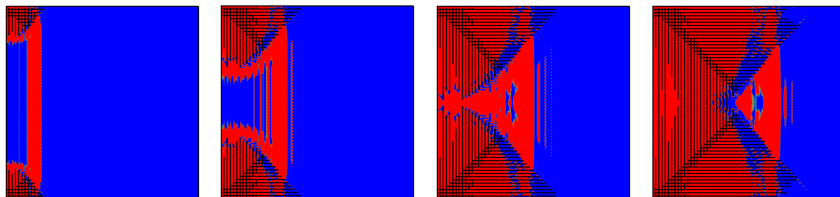
Crack propagation in a blocky medium

3 600 blocks each of them is 5×5 mm in size, between blocks – thin interlayers (0.05 mm)

Without initial stresses in the blocks



Level curves of the normal stress σ_{11}



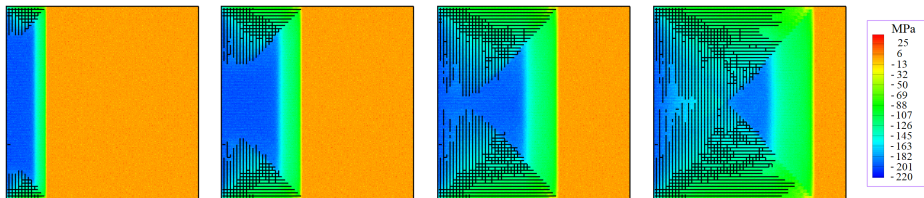
Plastic zones

Cracks in the interlayers are shown in **black** colour

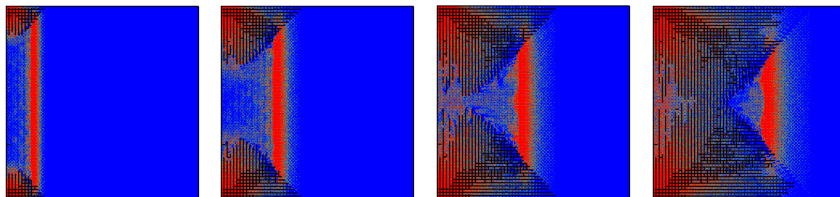
Crack propagation in a blocky medium

3 600 blocks each of them is 5×5 mm in size, between blocks – thin interlayers (0.05 mm)

Random distribution of initial stresses in blocks



Level curves of the normal stress σ_{11}



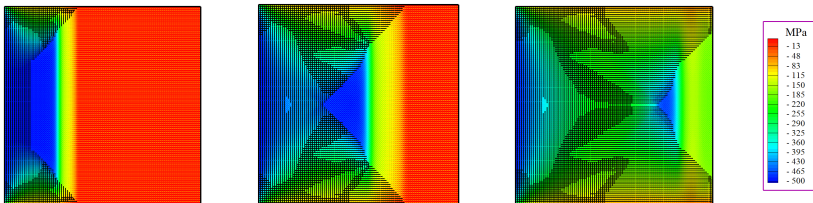
Plastic zones

Cracks in the interlayers are shown in **black** colour

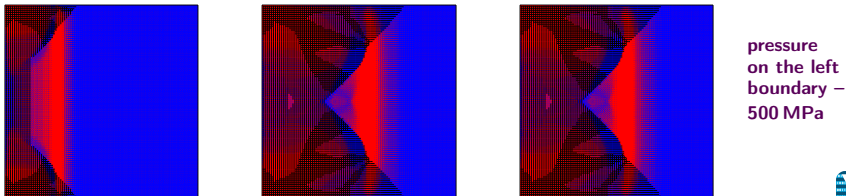
Crack propagation in a blocky medium

10 000 blocks each of them is 5×5 mm in size, between blocks – thin interlayers (0.05 mm)
 Total size of computational domain (taking into account the interlayers) is 50.5×50.5 cm

Self-balanced initial stresses inside each block



Level curves of the normal stress σ_{11}

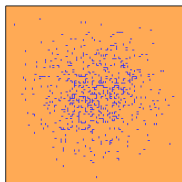
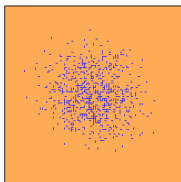
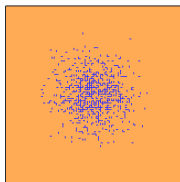
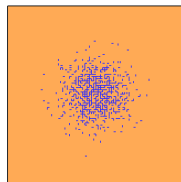
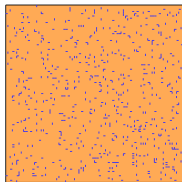
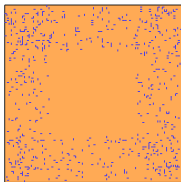
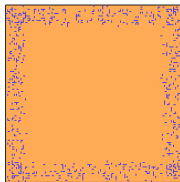
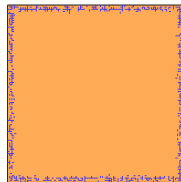


Plastic zones

Initial cracks in the interlayers between blocks

Possible variants of distribution of cracks in the interlayers – uniformly across the blocky massif, with a concentration in the center or along the borders of massif.

Computational domain consists of 80×80 blocks. Cracks are distributed randomly (5% concentration).


 $m = 3$

 $m = 5$

 $m = 7$

 $m = 9$

 $m = r = 1$

 $r = 2$

 $r = 5$

 $r = 25$

Random distribution of cracks in a blocky massif

Shock wave loading

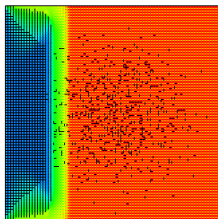
Prestressed blocky massif, consisting of 80×80 blocks (each block is self-balanced)

Each block is 0.625×0.625 mm in size, thin interlayers between them (0.025 mm)

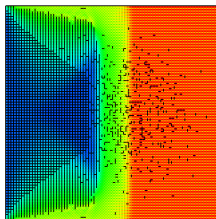
Total size of computational domain (taking into account the interlayers) is 5.2×5.2 cm

5 % system of cracks in the interlayers, concentration of cracks in the center of blocky massif ($m = 7$)

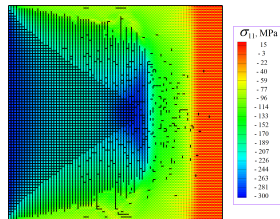
The wave motion is caused by the action of **uniformly distributed pressure $p = 300$ MPa** on the left boundary of the massif. Horizontal boundaries are free of stresses, right boundary is fixed.



$t = 3.38 \mu\text{s}$



$t = 6.75 \mu\text{s}$



$t = 10.13 \mu\text{s}$

Level curves of the normal stress σ_{11} and distribution of cracks in the blocky massif

Computations were performed on 80 processors of the cluster of ICM SB RAS.

Shock wave loading

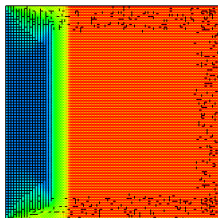
Prestressed blocky massif, consisting of 80×80 blocks (each block is self-balanced)

Each block is 0.625×0.625 mm in size, thin interlayers between them (0.025 mm)

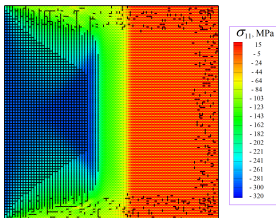
Total size of computational domain (taking into account the interlayers) is 5.2×5.2 cm

5% system of cracks in the interlayers, concentration of cracks along the borders of blocky massif ($r = 5$)

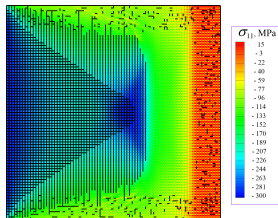
The wave motion is caused by the action of **uniformly distributed pressure $p = 300$ MPa** on the left boundary of the massif. Horizontal boundaries are free of stresses, right boundary is fixed.



$t = 3.38 \mu\text{s}$



$t = 6.75 \mu\text{s}$



$t = 10.13 \mu\text{s}$

Level curves of the normal stress σ_{11} and distribution of cracks in the blocky massif

Computations were performed on 80 processors of the cluster of ICM SB RAS.

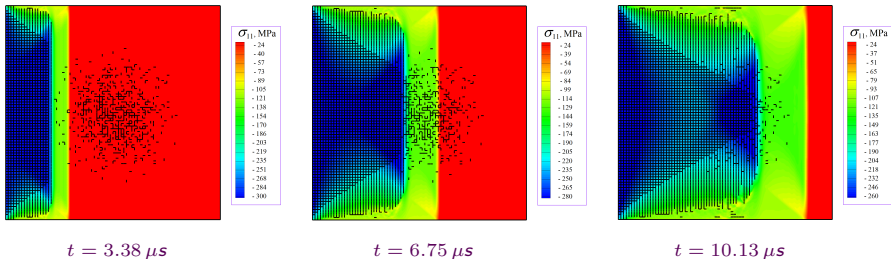
Shock wave loading

6 400 blocks each block is 0.625×0.625 mm in size, thin interlayers between them (0.025 mm)

Total size of computational domain (taking into account the interlayers) is 5.2×5.2 cm

Initial system of cracks in the interlayers, $m = 7$
(without initial stresses in the blocks)

The wave motion is caused by the action of **uniformly distributed pressure $p = 300$ MPa** on the left boundary of the massif. Horizontal boundaries are free of stresses, right boundary is fixed.



Level curves of the normal stress σ_{11} and distribution of cracks in the blocky massif

Computations were performed on 80 processors of the cluster of ICM SB RAS.

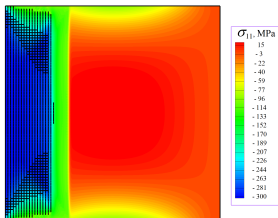
Shock wave loading

6 400 blocks each block is 0.625×0.625 mm in size, thin interlayers between them (0.025 mm)

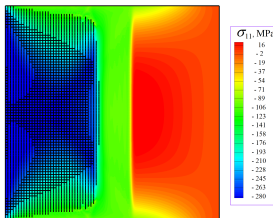
Total size of computational domain (taking into account the interlayers) is 5.2×5.2 cm

Self-balanced initial stresses throughout whole massif (without initial system of cracks in the interlayers)

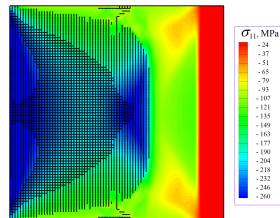
The wave motion is caused by the action of **uniformly distributed pressure $p = 300$ MPa** on the left boundary of the massif. Horizontal boundaries are free of stresses, right boundary is fixed.



$t = 3.38 \mu\text{s}$



$t = 6.75 \mu\text{s}$



$t = 10.13 \mu\text{s}$

Level curves of the normal stress σ_{11} and distribution of cracks in the blocky massif

Computations were performed on 80 processors of the cluster of ICM SB RAS.

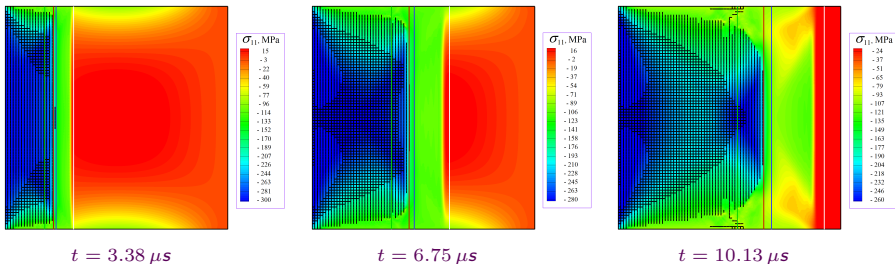
Finding the velocity of fracture wave

$C_p = 4750$ m/s – velocity of longitudinal elastic shock wave

$C_s = 2750$ m/s – velocity of transverse elastic shock wave

$C_f = \sqrt{C_p^2 - 4C_s^2/3} \approx 3533$ m/s – velocity of plastic shock wave

$C_{fr} \approx 0.95 C_f = 3356$ m/s – velocity of fracture wave



Level curves of the normal stress σ_{11} and distribution of cracks in the blocky massif

White line corresponds to the longitudinal elastic shock wave,
 green line – to the transverse elastic wave, blue line – to the plastic wave,
 and red line corresponds to the fracture wave.

Dynamic loading

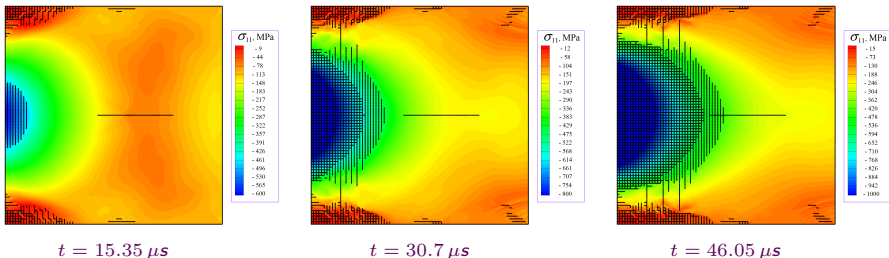
6 400 blocks each block is 0.625×0.625 mm in size, thin interlayers between them (0.025 mm)

Total size of computational domain (taking into account the interlayers) is 5.2×5.2 cm

Self-balanced initial stresses throughout whole massif

The pressure on left boundary of the massif is changed gradually from the center to corners (maximum – in the center), pressure increases with time.

Upper and lower boundaries of computational domain are free of stresses, right boundary is fixed.



Level curves of the normal stress σ_{11} and distribution of cracks in the blocky massif

Computations were performed on 80 processors of the cluster of ICM SB RAS.

Dynamic loading

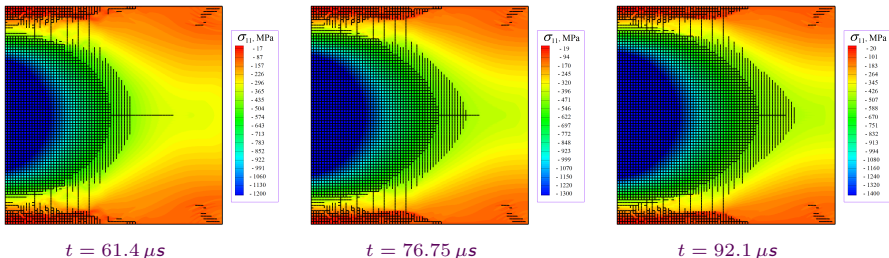
6 400 blocks each block is 0.625×0.625 mm in size, thin interlayers between them (0.025 mm)

Total size of computational domain (taking into account the interlayers) is 5.2×5.2 cm

Self-balanced initial stresses throughout whole massif

The pressure on left boundary of the massif is changed gradually from the center to corners (maximum – in the center), pressure increases with time.

Upper and lower boundaries of computational domain are free of stresses, right boundary is fixed.



Level curves of the normal stress σ_{11} and distribution of cracks in the blocky massif

Computations were performed on 80 processors of the cluster of ICM SB RAS.

Dynamic loading

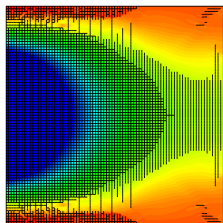
6 400 blocks each block is 0.625×0.625 mm in size, thin interlayers between them (0.025 mm)

Total size of computational domain (taking into account the interlayers) is 5.2×5.2 cm

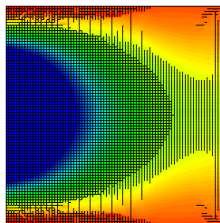
Self-balanced initial stresses throughout whole massif

The pressure on left boundary of the massif is changed gradually from the center to corners (maximum – in the center), pressure increases with time.

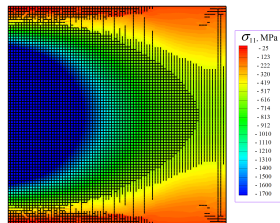
Upper and lower boundaries of computational domain are free of stresses, right boundary is fixed.



$t = 107.46 \mu\text{s}$



$t = 122.81 \mu\text{s}$

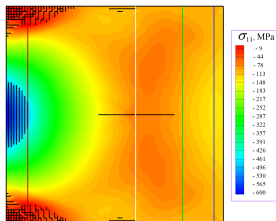


$t = 138.16 \mu\text{s}$

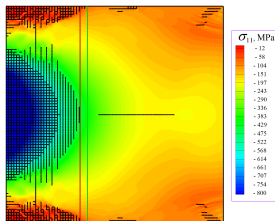
Level curves of the normal stress σ_{11} and distribution of cracks in the blocky massif

Computations were performed on 80 processors of the cluster of ICM SB RAS.

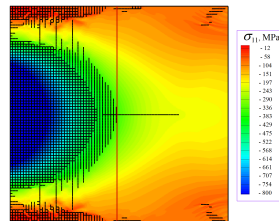
Finding the velocity of fracture wave



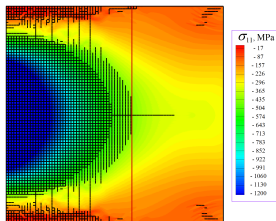
$C_{fr} = 343 \text{ m/s}$ ($t = 15.35 \mu\text{s}$)



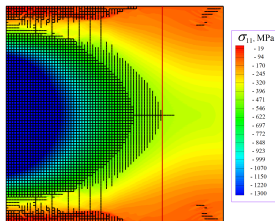
$C_{fr} = 578 \text{ m/s}$ ($t = 30.7 \mu\text{s}$)



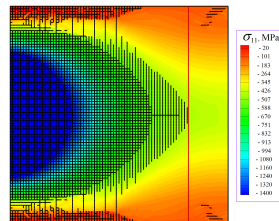
$C_{fr} = 554 \text{ m/s}$ ($t = 46.05 \mu\text{s}$)



$C_{fr} = 491 \text{ m/s}$ ($t = 61.4 \mu\text{s}$)



$C_{fr} = 487 \text{ m/s}$ ($t = 76.75 \mu\text{s}$)



$C_{fr} = 461 \text{ m/s}$ ($t = 92.1 \mu\text{s}$)



Conclusion



- A new efficient numerical method is proposed for analyzing the wave nature of propagation of a system of cracks in thin interlayers of a blocky medium with complex rheological properties.
- The method is based on a variational formulation of the constitutive relations for deformation of elastic-plastic and porous materials, as well as the conditions of contact interaction of blocks through interlayers.
- Self-balanced preliminary stresses are taken into account in blocks, the stored energy of which is released as plastic loading waves pass through. This ensures a self-sustaining mechanism of material fragmentation along the interlayers with formation of a fracture wave front.
- Parallel computational algorithm is developed that implements this method for supercomputers with cluster architecture.
- The results of numerical simulation of the fracture waves propagation in tempered glass under the action of dynamic disturbances are presented.

This work is supported by the Krasnoyarsk Mathematical Center and financed by the Ministry of Science and Higher Education of the Russian Federation in the framework of the establishment and development of regional Centers for Mathematics Research and Education (Agreement No. 075-02-2026-735)

